Polymer 279 (2023) 126021

Contents lists available at ScienceDirect

Polymer

journal homepage: www.elsevier.com/locate/polymer

Uncharted development of electrospun mats based on bioderived poly (butylene 2,5-furanoate) and poly(pentamethylene 2,5-furanoate)

Sofia Santi [a,1], Michelina Soccio [c,d,1], Giulia Fredi [a,*], Nadia Lotti [c,d,e], Andrea Dorigato [a]

[a] Department of Industrial Engineering and INSTM Research Unit, University of Trento, Via Sommarive 9, 38123, Trento, Italy
[c] Department of Civil, Chemical, Environmental, and Materials Engineering, University of Bologna, Via Terracini 28, 40131, Bologna, Italy
[d] Interdepartmental Center for Industrial Research on Advanced Applications in Mechanical Engineering and Materials Technology, CIRI-MAM, University of Bologna, Bologna, Italy
[e] Interdepartmental Center for Agro-Food Research, CIRI-AGRO, University of Bologna, Bologna, Italy

ARTICLE INFO

Keywords:
Biopolymers
2,5-Furandicarboxylic acid
poly(butylene 2,5-furanoate)
poly(pentamethylene 2,5-furanoate)
Electrospinning
Fibers
Rheological properties

ABSTRACT

Sustainable and bioderived furanoate polyesters are emerging as promising substitutes for petrochemical-derived polyesters, which are mainly applied in packaging, textile, and biomedical fields. This work presents the successful production, for the first time, of electrospun nanofibrous mats based on two furan-based polyesters, i.e., poly(butylene 2,5-furanoate) (PBF) and poly(pentamethylene 2,5-furanoate) (PPeF), which have very similar chemical structure but remarkably different physical and mechanical properties. The feasibility to produce nanofibrous mats of PBF and PPeF by electrospinning was systematically investigated, by optimizing (i) the solubility of the polymers in different solvent mixtures, (ii) the viscosity and concentration of the spinning dopes, evaluated through rheological measurements of the polymeric solutions, (iii) the spinning rate, and (iv) the applied voltage. A detailed morphological analysis of the resulting non-vowen mats, carried out through field-emission scanning electron microscopy (FESEM), allowed the screening of the best processing conditions for PBF and PPeF, in order to produce electrospun mats suitable for biomedical applications.

1. Introduction

The recent increasing difficulties of plastics disposal have raised concerns worldwide. Most of the plastics waste ends up in landfills, oceans, soil and water, representing a serious hazard for plants, animals and humans. According to recent statistics, every year up to 12.7 million tons of plastics enter the oceans, causing the death of several seabirds and aquatic animals. The extent of this problem will exponentially increase with the increase in global fossil-based plastics consumption [1–3]. As forecasted by the OECD's Global Plastic Outlook, plastics waste is estimated to triple by 2060, passing from 353 million tons in 2019 to 1014 million tons in the next decades [4]. Therefore, effective alternatives must be detected to avoid irreversible consequences on ecosystems and human beings. Nowadays, bioplastics have become a topic of great interest as a possible solution to overcome the issues related to fossil-based polymeric waste [5–8].

The global bioplastics production capacity is expected to increase from about 2.4 million tonnes in 2021 to approximately 7.6 million tonnes in 2026, as demonstrated by the market data compiled by European Bioplastics in cooperation with the Nova Institute [9]. The bio-based alternatives to petroleum-derived plastics include renewable polymeric materials derived from biomasses through eco-sustainable processes, helping to reduce the current environmental pollution. In particular, great interest has been recently raised in poly(alkylene 2,5-furanoate)s (PAFs), bio-based polyesters synthesized starting from 2,5-furandicarboxylic acid (FDCA) and glycols with a variable alkyl chain length [10–13].

Recent studies on PAFs showed that they have very good thermal stability as well as better thermo-mechanical and gas barrier properties than their oil-based terephthalic counterparts [14]. Moreover, the presence of a polar furan ring in their chemical structure makes PAFs more hydrophilic and easily attackable by microorganisms, and thus potentially more compostable compared to poly(alkylene terephthalate)s, which contain a non-polar benzene ring [15]. Among PAFs, Poly (ethylene 2,5-furandicarboxylate) (PEF) is the most studied furan-based thermoplastic polyester and it is considered an excellent biobased

* Corresponding author.
E-mail address: giulia.fredi@unitn.it (G. Fredi).
[1] These authors contributed equally.

https://doi.org/10.1016/j.polymer.2023.126021
Received 14 April 2023; Received in revised form 10 May 2023; Accepted 12 May 2023
Available online 12 May 2023

alternative to poly(ethylene terephthalate) [16–20]. More recently, poly (butylene 2,5-furandicarboxylate) (PBF) [21,22] and poly(pentamethylene furanoate) (PPeF) [23–25] have been considered very promising materials for different applications.

PBF and PPeF have very similar repeating unit that differs in just one methylene group, but they have remarkably different physical and mechanical properties. PBF can be synthesized by melt polycondensation of 2,5-furandicarboxylic acid (FDCA) or dimethyl 2,5-furandicarboxylate (2,5-DMF) with butylene glycol (BD) [22]. During condensation polymerization, organometallic compounds such as titanium alkoxides are used as catalysts, to accelerate the polymerization and produce high molecular weight products. Titanium alkoxides are emerging as important poly-esterification catalysts due to their high activity, non-toxic and environmental safety [26]. PBF shows similar thermo-mechanical properties to poly(butylene terephthalate) (PBT), but it presents a lower processing temperature and improved ductility, with a glass transition (T_g) at 33–35 °C and a melting point (T_m) at approx. 172 °C. On the other hand, PPeF can be synthesized through a two-stage polycondensation synthesis similarly to the PBF, with 1,5-pentanediol (PD) instead of BD [25]. Thus, PPeF contains a diol with five carbon atoms that significantly affects the thermo-mechanical properties of PPeF, resulting in a lower T_g, 17 °C, a more ductile behavior, and elevated elongation at break. Unlike PBF, PPeF is amorphous, as commonly found for C-odd-numbered glycolic subunits, and exhibits a crystallization kinetics of months [27].

Both PBF and PPeF have been recently processed as films by compression moulding [22,28] as fibers [27] and as a blend with PLA and other biobased polymers [29,30]. However, further physical, mechanical, and rheological studies will be needed to provide a more comprehensive understanding of the potential of these materials for other applications. For instance, it could be interesting to employ both PBF and PPeF electrospun mats in the biomedical field or filtration systems. Electrospinning has arisen as a promising technique in the field of nanofiber fabrication starting from a wide variety of materials. This simple and highly effective technique has found its application in different areas, but the process is typically limited to identifying the operating conditions for producing fibers with suitable properties. In particular, PBF might be a promising alternative to PBT, widely applied in electrospun mats for blood filtration [31] or for tissue regeneration in blend with poly(ethylene oxide terephthalate) [32]. On the other hand, electrospun PPeF mats might be used for seals or membranes and separators for batteries.

Therefore, the aim of this work is to systematically evaluate the feasibility of producing, for the first time, nanofibrous mats of PBF and PPeF by electrospinning. The main factors considered in this study for PBF and PPeF mats formation by electrospinning were the following: (i) viscosity and concentration of the spinning dope, (ii) volatility and miscibility in water of the solvent, (iii) solubility of the polymers in different solvents, (iv) spinning rate and voltage and (v) the thermal stability of the polymers at temperature and humidity constant, respectively at 20 °C and 45%. A detailed morphological analysis through field emission scan electron microscopy (FESEM) allowed the screening of the best spinning conditions both for PBF and PPeF matrices. The screening was based on the evaluation of (i) the absence of beads in the mats and (ii) the mats' homogeneity, in terms of uniformity of the fiber size. Moreover, the contact angle was also evaluated on the optimized PBF and PPeF mats, in order to determine their wettability and their suitability for cell adhesion in case of biomedical application.

2. Materials and methods

2.1. Materials

Dimethyl 2,5-furandicarboxylate (2,5-DMF) (2,5-DMF) (Sarchem labs, CAS 4282-32-0), 1,4-butanediol (1,4-BDO) (Sigma-Aldrich, 99% pur, CAS 110-63-4), 1,5-pentanediol (1,5-PD) (Fluka, ~97% pur, CAS 111-29-5), Hexafluoroisopropanol (Carlo Erba/Cas 920-66-1, Hexafluoro-2-propanol, HFIP), Chloroform (Carlo Erba/Cas 67-66-3, Chloroform, $CHCl_3$), dimethylformamide (Sigma/Cas 68-12-2, DMF).

PBF and PPeF synthesis. Poly(butylene 2,5-furanoate) (PBF) and poly(pentamethylene 2,5-furanoate) (PPeF) were synthesized at the lab scale through a solvent-free polycondensation process, according to the procedure described in the works of Guidotti et al. [25] starting from dimethyl 2,5-furandicarboxylate (2,5-DMF) and glycols, 1,4-butanediol (1,4-BDO) for PBF, 1,5-pentanediol (1,5-PD) for PPeF and titanium tetrabutoxide (TBT) and titanium isopropoxide (TIP) used as catalysts [29]. The chemical formulas of PBF and PPeF are reported in Scheme 1.

2.2. Sample preparation

2.2.1. Preparation and composition of the spinning dopes

PBF and PPeF flakes were dissolved at 0.1 or 0.2 g/mL in different solvents (HFIP, $CHCl_3$, DMF), generally used in the electrospinning process for their volatility, conductivity and solubility properties [33,34] at different relative concentrations, as reported in Table 1.

From each sample, 2 mL solution was collected in a borosilicate syringe used for the electrospinning process. Furanoate-based mats were produced by changing the set-up of the processing parameters (spinning rate and voltage) and solution conditions, but maintaining the temperature and the humidity constant, respectively at 20 °C and 45%.

2.2.2. Preparation of PBF and PPeF non-woven mats

The electrospinning setup, reported in Fig. 1, was fixed in a poly (methyl methacrylate) (PMMA) chamber with controlled temperature and humidity. The electrostatic forces were obtained by applying an electrical field by means of a DC voltage source of 18 kV or 24 kV and a distance of 15 cm between the nozzle tip and a flat aluminum foil, utilized as a collector. On the other hand, different spinning rates, between 0.01 and 0.2 mL/min, were obtained by means of a syringe pump able to regulate the flow of the solution from the nozzle, which had a diameter of 0.9 mm.

2.3. Experimental techniques

2.3.1. Thermal properties of the as-synthetized PBF and PPeF

Thermal properties of the as-synthetized PBF and PPeF were evaluated through differential scanning calorimetry (DSC), performed with a Mettler DSC 30 calorimeter (Mettler Toledo, Inc.). About 12 mg of the as-synthesized PBF and PPeF was placed in an aluminum pan with a capacity of 40 μL and subjected to the following thermal program: 1st heating of 10 °C/min in a temperature range from −50 to 200 °C, a cooling from 200 °C to −50 °C and a 2nd heating from −50 to 200 °C under a nitrogen flow of 100 mL/min. The glass transition temperature (T_g) was calculated as the midpoint of the glass-to-rubber transition step. The melting temperature (T_m) and the cold crystallization temperature (T_{cc}) were determined as the peak maximum/minimum of the endothermic/exothermic phenomena in the DSC curve, respectively. The corresponding heat of fusion (ΔH_m) and heat of crystallization (ΔH_c) were obtained from the total area of the endothermic and exothermic signals, respectively.

The degree of crystallinity was also evaluated considering the enthalpy of melting of fully crystalline PBF ($\Delta H_m{}^0$), taken as 129 J/g [15] and applying Equation (1), [35]

$$X_{-}(c) = \Delta H_{-}(m) \; / \Delta H_{-}(m)\,(\hat{0}) \tag{1}$$

2.3.2. Rheological properties of PPeF and PBF solutions

The rheological properties of the solutions reported in Table 1 were analyzed using an ARES torsional rheometer (TA Instruments Discovery HR-2 Hybrid). The viscosity of the spinning dopes is a very important parameter that determines their spinnability. Dynamic rheological measurements were conducted in an angular frequency range from

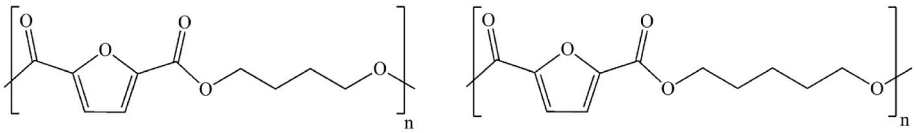

Poly(butylene 2,5-furanoate) PBF Poly(pentamethylene 2,5-furanoate) PPeF

Scheme 1. Chemical formulas of PBF and PPeF.

Table 1
PBF and PPeF solutions prepared for electrospinning, with the type of solvents used and the nominal concentrations.

Samples	Concentrations g/mL	Solvents	Abbreviation
PBF	0.1	H	H
	0.2	H/C in ratio 7:3	H/C (7/3)
PPeF	0.1	H/C in ratio 1:1	H/C (1/1)
	0.2	D/C in ratio 1:9	D/C (1/9)
		D/C in ratio 1:5	D/C (1/5)

H = HFIP, C = $CHCl_3$, D = DMF.

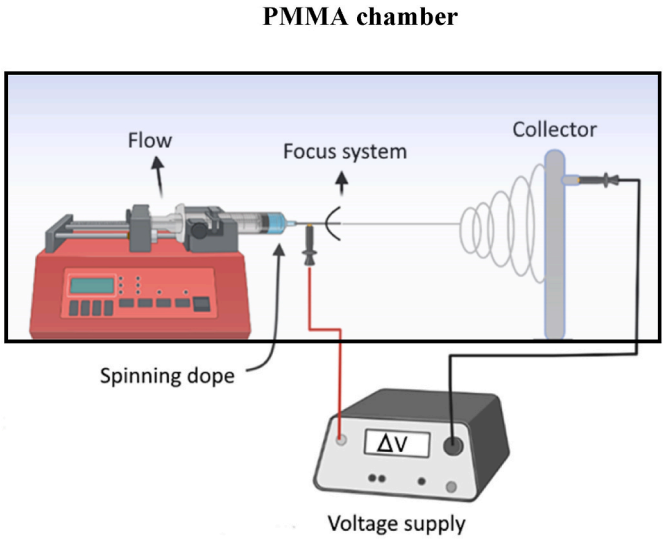

Fig. 1. Representative image of the lab made electrospinning set up for the preparation of PPeF and PBF non-woven mats.

10^{-2}–10^{2} rad/s under atmospheric pressure. The analysis was carried on at 20 °C on 1000 μL of each solution, by using a cone-plate geometry covered with an evaporation blocker and a strain amplitude of 5% for the evaluation of viscosity.

2.3.3. Surface characterization of the electrospun mats

The microstructural features of the electrospun mats were investigated by using a Zeiss Supra 60 (Carl Zeiss AG) field emission microscope (FESEM), operating at an acceleration potential of 2.5–3.5 kV. Before the observations, the samples were sputtered with a platinum–palladium coating for 20 s, to render them conductive. The FESEM images were analyzed by ImageJ® software to determine the fiber diameter distribution and screen the optimal conditions for the PPeF and PBF mat formation.

Whereas, the surface properties (i.e. the wettability) of the PBF and PPeF mats with a thickness of about 4 μm, were evaluated through contact angle measurements, performed with a Dino-Lite Edge Handheld Digital Microscope/Camera at 25 °C. The side profiles of deionized water drops previously deposited on the surface of the mat were acquired and analyzed 5 s after deposition. The tests were performed on three different areas for each sample), to obtain the mean water contact angle (WCA) values.

3. Results and discussion

3.1. Thermal properties of the as-synthesized PBF

The thermal analysis by DSC of as-synthesized PBF was performed to evaluate the thermal properties and purity after the synthesis. As reported in the thermograms in Fig. 2(a) and in the results of Table 2, the first heating scan shows the T_g of PBF at 34 °C, whereas the T_g of the second heating shifts at 39 °C that it might be caused by the presence of water absorbed still in the material during the first heating scan [36]. The T_g is followed by a melting peak at 175 °C, with ΔH_m of 65.1 J g^{-1}. Moreover, the degree of PBF crystallinity was also evaluated at 50% (see Table 3).

3.2. Thermal properties of the as-synthesized PPeF

DSC was also performed, for the same reasons, on as-synthesized PPeF. PPeF results as a fully amorphous polymer, as reported in Fig. 2 (b); the T_g is observed at 16 °C in the first heating scan. Indeed, the C-odd number of the glycolic subunit affects the capacity of PPeF to crystalize, while the longer aliphatic subunit provides an increase in molecular mobility and ductility.

The T_g definition for amorphous polymers is an important parameter that should be preliminarily considered for the electrospinning process, as above T_g the polymers will start flowing. Moreover, an amorphous polymer with a T_g near the room conditions generally produces fused fiber webs [37] during the electrospinning process. This phenomenon is, generally, due to inappropriate environmental conditions, spinning distance, or solvents used [33] that cause an incomplete fiber formation before hitting the collector. Thus, the glass-to-rubber transition of the PPeF amorphous domains below room temperature has made challenging the definition of the optimal electrospinning parameters.

3.3. Rheology of PBF solutions

PBF flakes were dissolved utilizing different solvent mixtures based on DMF, HFIP and $CHCl_3$ as described in Table 1, generally used in the electrospinning process, for their volatility, conductivity and solubility properties [33,34]. The solubility of PBF was evaluated for each solution by visual observations and it can be concluded that the PBF is well dispersed in all the mixtures except for the mixture with a D/C ratio 1/9 and 1/5, where PBF results insoluble and thus unsuitable for the electrospinning process. Indeed, the presence of crystalline phase and glassy domains prevents the diffusion of solvent and, additionally, the solubility is affected by the hydrogen bonding capability of the solvent that is weak for hydrocarbons, chlorinated hydrocarbons (such as $CHCl_3$) and nitrohydrocarbons [38].

The results of rheological tests on the prepared PBF solutions are reported in Fig. 3(a). The trends of viscosity reveal a shear thinning behavior from 0.01 to 20 Hz, which is typical of non-newtonian fluids, whose viscosity decreases with the shear strain reaching the equilibrium at higher shear rates. In particular, the PBF solutions in the range of viscosity values around 0.13–0.08 Pa s result suitable for the electrospinning process as demonstrated by FESEM images. Indeed, at these values it was observed the formation of the Taylor cone and the

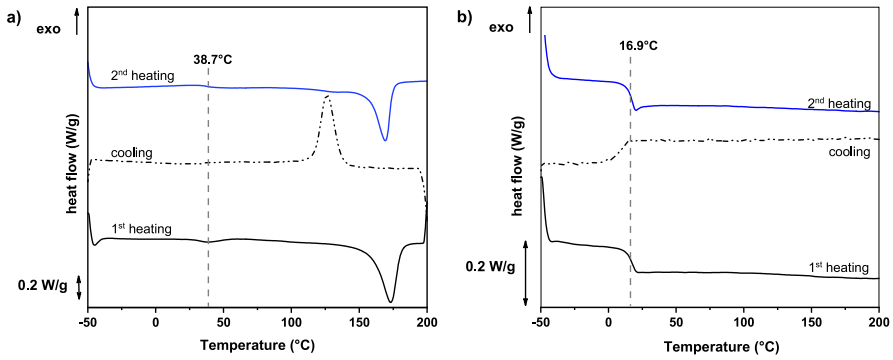

Fig. 2. DSC thermograms of the as-synthesized (A) PBF and (B) PPeF.

Table 2
Results of DSC tests on as-synthesized PPeF and PBF.

	M_n g/mol	D	1st heating scan				2nd heating scan			
			T_g °C	ΔC_p J/g°C	T_m °C	ΔH_m J/g	T_g °C	ΔC_p J/g°C	T_m °C	ΔH_m J/g
PBF	36500	2.2	39	0.18	175	61.3	34	0.19	175	65.1
PPeF	43900	2.3	16	0.46	/	/	15	0.44	/	/

Table 3
Summary of viscosity values.

Samples	Concentration (g/mL)	Solvents	Viscosity (Pa•s)
PBF	0.2	H	0.87
		H/C (7/3)	0.72
		H/C (1/1)	0.63
	0.1	H	0.08
		H/C (7/3)	0.11
		H/C (1/1)	0.13
PPeF	0.2	H	1.01
		H/C (7/3)	0.87
		H/C (1/1)	0.5
		D/C (9/1)	0.18
		D/C (5/1)	0.17
	0.1	H	0.20
		H/C (7/3)	0.11
		H/C (1/1)	0.06
		D/C (9/1)	0.03
		D/C (5/1)	0.04

deposition of smooth fibers on the collector.

3.4. Rheology of PPeF solutions

PPeF flakes were also dissolved utilizing the same solvent mixtures for the PBF dissolution, described in Table 1, and the solubility of PPeF was evaluated by visual observations for each solution, where the PPeF is well dispersed in all the mixtures.

The results of rheological tests on prepared solutions are reported in Fig. 3(b). The viscosity of PPeF solutions in the narrow range of values around 0.2–0.17 Pa s results suitable for the electrospinning process as demonstrated by FESEM images. In particular, that is observed for the PPeF dissolved in HFIP at 0.1 g/mL and for PPeF dissolved in D/C (1/5) and (1/9) at 0.2 g/mL.

In the same solvent and concentration conditions, the two homopolymers show similar behavior. The solutions above 0.2–0.17 Pa s do not allow the formation of the Taylor cone and the deposition of smooth fibers on the collector as well as the values below promote the formation of beads.

3.5. Morphological characterization of the electrospun mats made of PBF

Each solution of PBF described in Section 3.2 was tested to be submitted to the electrospinning process at different spinning rates and voltages, to prepare mats. In particular, the 0.2 g/mL PBF solutions resulted not spinnable due to the high viscosity, whereas the mats produced by the electrospinning of H, H/C (7/3), H/C (1/1) solutions based on 0.1 g/mL PBF extruded at 0.01–0.05–0.1 mL/min and with a voltage of 18 kV or 24 kV were efficiently formed and, thus, investigated by FESEM and WCA analysis. In this paper, only the results on the mats performed at 24 kV are reported, because a voltage of 18 kV produced fibers of higher diameter or with the presence of beads.

As reported in Fig. 4, the FESEM images highlight the morphology of the mats based on PBF.

The distributions of the fiber diameter for the mats produced by the electrospinning are summarized in Table 4.

In particular, the H/C (1/1) sample at 0.01 mL/min shows smooth fibers of 0.8 ± 0.2 μm in diameter as well as the H/C (7/3) samples, that show an increase in the diameter of the fibers from 1.0 ± 0.2 μm to 2.0 ± 0.2 μm increasing the spinning rate. The other compositions show a non-homogeneous distribution of fibers and the presence of beads. Moreover, the fibers decrease in diameter while reducing the spinning rate, as well as decreasing the HFIP content the fibers appear more homogenous at low spinning rates.

Once set the conditions for the electrospinning of the PBF solutions at 24 kV and 0.01 mL/min, an optimization of the concentrations was also performed to reach a good compromise between a homogeneous distribution of fibers and low fiber diameter. From the FESEM images reported in Fig. 5, the PBF solution in H/C (1/1) at a concentration of 0.11 g/mL generates more homogeneous fibers than other compositions. Indeed, through dimensional analysis, it is possible to determine a mean fiber size of i) 0.8 ± 0.4 μm for the PBF solution of 0.1 g/mL, ii) 0.7 ± 0.3 μm for the PBF solution of 0.11 g/mL and iii) 1.5 ± 0.3 μm for PBF of 0.125 g/mL. Thus, as expected from a preliminary visual observation, the PBF 0.11 g/mL sample shows a more homogeneous distribution of fiber mainly in the submicrometer range, resulting as the optimized PBF solution at the fixed electrospinning parameters.

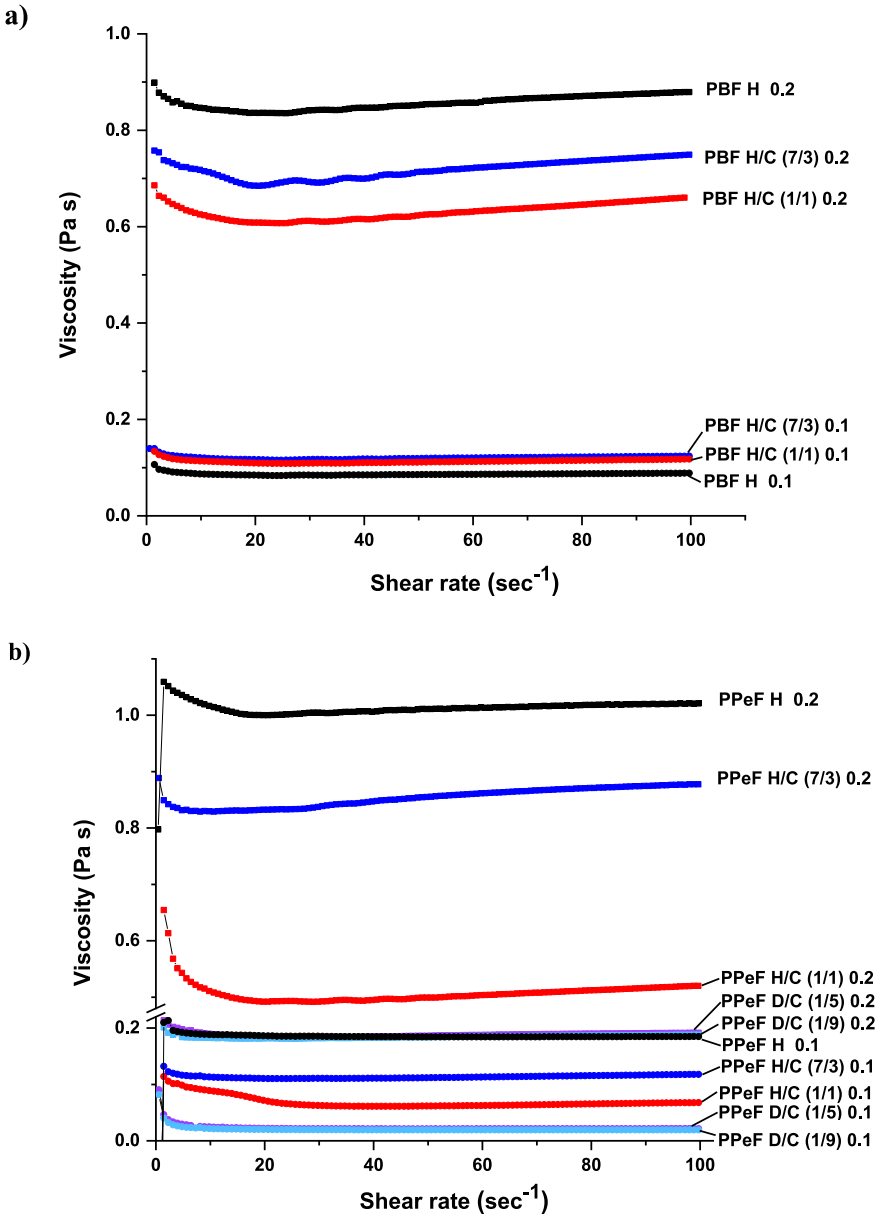

Fig. 3. Results of the dynamic rheological tests on the prepared solutions. Viscosity of (a) PBF and (b) PPeF solutions (D:DMF, H: HFIP, C: $ClCH_3$) at 0.2 or 0.1 mg/mL as a function of the shear rate.

3.6. Morphological characterization of the electrospun mats made of PPeF

The morphological characterization of PPeF mats was also performed through FESEM analysis. In particular, 0.1 g/mL PPeF H/C (7/3), H/C (1/1), D/C (1/5) and D/C (1/9) solutions produce droplets mats, whereas the mats produced by using 0.2 g/mL PPeF H, H/C (7/3), H/C (1/1), D/C (1/9) solutions show fibers completely fused, thus these images are not reported.

Only the 0.1 g/mL PPeF H solution efficiently produces mats at different spinning rates of 0.01–0.05–0.1 mL/min and 24 kV or 18 kV and are, thus, analyzed by FESEM and WCA analysis.

The FESEM images of samples show fibers slightly fused with a mean size of 1.0 ± 0.8 μm for the H-based solution, as reported in Fig. 6(a), becoming completely fused with the increase of chloroform content, as reported in Fig. 6(b). As previously assumed, the electrospinning of the PPeF results in a fused web due to the fact that the electrospinning has been performed close to the T_g of PPeF. FESEM images report only mats derived from the PPeF solutions in HFIP, whereas the incremental $CHCl_3$ content decreases the viscosity, as reported in Section 3.4, which leads, together with the environmental conditions near the T_g of PPeF, to completely fused fibers. The formation of fused webs might be prevented by changing the solvent mixture. Thus, the content of DMF, which has a high boiling point, conductivity, and high dielectric constant and is generally used to produce smooth electrospun fibers was increased with a D/C ratio of 1:5 (D/C (1/5)), as reported in Fig. 6(c). The DMF added to $CHCl_3$ as a co-solvent increases the conductivity and reduces the volatility of the solution, and increases the electrospinnability of the polymer solution. The higher conductivity would lead to a higher charge capacity of the solution and a consequent increase in the stretching force on the jet spray allowing the fiber formation [39].

The parameters for the electrospinning of PPeF solutions were fixed at a concentration of 0.2 g/mL and spinning parameters of 24 kV, 0.1 mL/min. The higher amount of DMF results in better fiber formation by

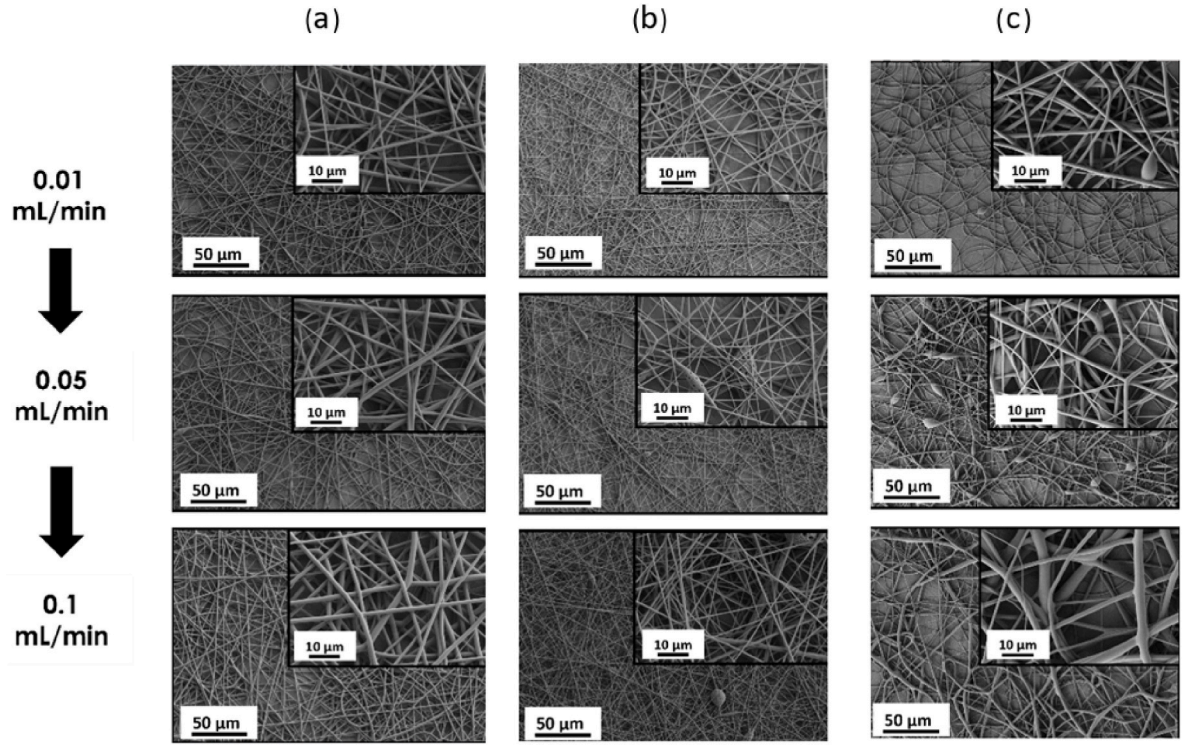

Fig. 4. FESEM analysis of PBF mats obtained at different spinning rates and applying different solvent mixtures. (a) H/C (7:3), (b) H/C (1:1), (c) H.

Table 4
Summary of PBF fibers distribution by varying the spinning rate.

Samples	Concentration (g/mL)	Spinning rate (mm/min)	Solvent	Fiber diameter (μm)
PBF	0.1	0.01	H	1.3 ± 0.4
			H/C (7/3)	1.1 ± 0.2
			H/C (1/1)	0.7 ± 0.2
		0.05	H	1.9 ± 0.7 μm
			H/C (7/3)	1.3 ± 0.3 μm
			H/C (1/1)	0.9 ± 0.2 μm
		0.1	H	2.2 ± 0.9 μm
			H/C (7/3)	1.7 ± 0.3 μm
			H/C (1/1)	1.5 ± 0.2 μm

keeping the effect of the temperature in the background. Indeed, the PPeF fibers of D/C (1/5) samples have an average diameter of 1.3 ± 0.6 μm, whereas the fibers of the D/C (1/9) sample cannot be defined. It is known from the literature that the conductivity of the polymer solution might be the key factor for the production of electrospun PPeF fibers [34]. Indeed, smooth fibers are generally produced by using a hydrophobic polymer dissolved in a water-miscible and little volatile solvent [40] as is DMF.

The optimized PPeF and PBF mats were also further characterized to evaluate their wettability through CA measurements. In fact, it is well known that the surface wettability does not depend only on the chemical composition but also on the microstructure and morphology [41]. Hence, it is important to assess the wettability of the prepared mats as a function of the combination between their chemistry and morphology. As reported in Fig. 7, the CA values result in 130° for PBF, 90° for PPeF in D/C (1/5), and 75° for PPeF in H, highlighting an increase of wettability in PPeF mats with respect to PBF mats. This increase is due to the residual presence of solvent in PPeF mats, as demonstrated by the WCA analysis on the same PPeF mats after the complete removal of the solvent under vacuum overnight. The former processing step results are fundamental for future biomedical applications to avoid cytotoxicity phenomena. After the treatment, CA values result of 130° for each sample while being present different roughness on the surface of the drop contact. Thus, the high hydrophobicity might result in difficult cell adhesion and need surface modification. For this reason, the application of PBF or PPeF mats as dermal patches might be preferable. Moreover, these mats could be suitable for the dispersion of non-polar active ingredients, thus difficult to administer by water.

4. Conclusions

In the present work, the production of nanofibrous mats of PBF and PPeF by electrospinning was systematically evaluated. For the first time, the electrospinning of PBF and PPeF was deeply investigated as a function of several parameters: (i) solubility of the polymers in suitable solvent mixtures, (ii) viscosity and concentration of the solutions, and (iii) processing parameters such as the spinning rate and voltage. From DSC analysis, the as-synthetized PBF and PPeF showed a T_g near the room temperature, at 39 °C and 16 °C, respectively. Moreover, PBF is semicrystalline. As a consequence, the glassy state and the semicrystalline structure of PBF prevent the agglomeration of fibers while working at room temperature, whereas, the rubbery state of PPeF, fully amorphous, is sensitive to the environmental condition resulting in fused fibers. The PPeF and PBF solutions were evaluated in terms of solubility in different solvents and rheological behavior. In particular, PBF resulted insoluble in D/C mixture and soluble in the other combinations of solvents, whereas PPeF was soluble in all the considered conditions. The viscosity of each solution was also evaluated and a range of values between 0.13 and 0.08 Pa s of PBF solutions and a narrow range around 0.2–0.17 Pa s for 0.1 mg/mL PPeF H and 0.2 mg/mL PPeF D/C (1/5) and D/C (1/9) solutions were considered suitable for electrospinning.

The FESEM images showed that the PPeF mats derived from the H

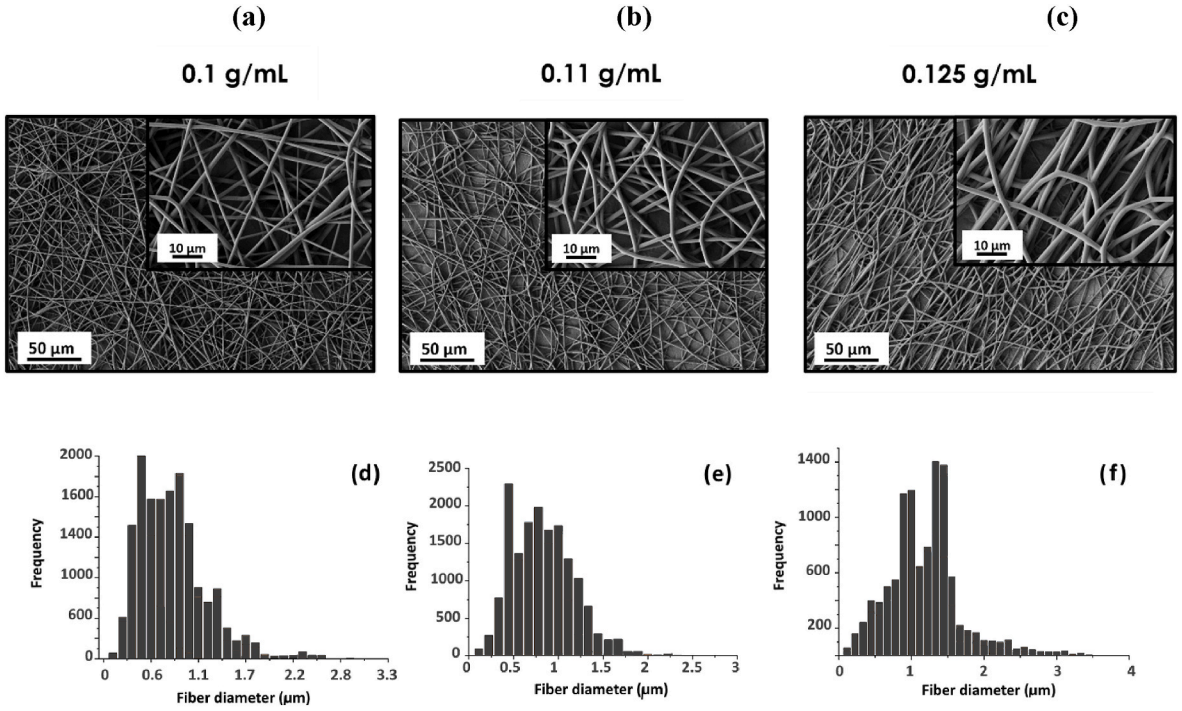

Fig. 5. FESEM images of the PBF electrospun mats prepared by using PBF in H/C (1:1) solutions. PBF concentraton of (A) 0.1 g/mL, (B) 0.11 g/mL, (C) 0.12 g/mL and their fiber diameter distribution (d, e, f).

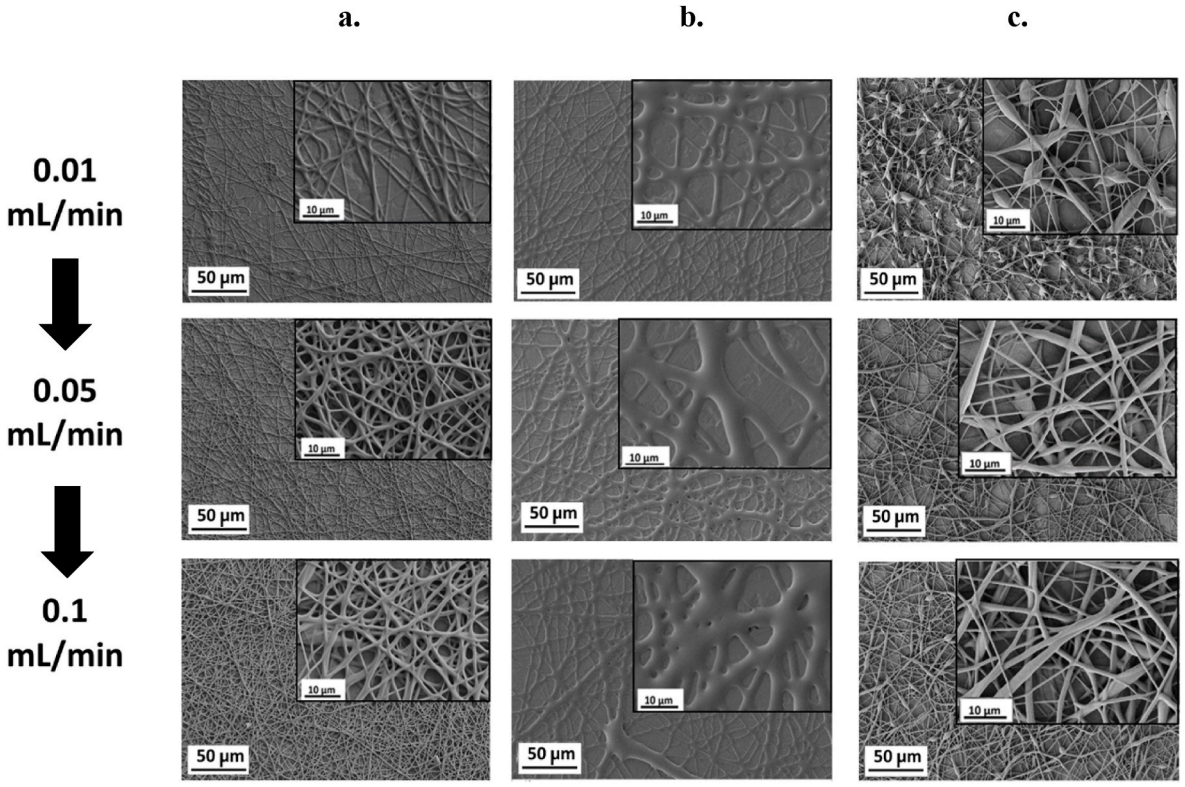

Fig. 6. FESEM images of the PPeF electrospun mats prepared by using PPeF in (a) H solvent, (b) D/C 1:9, (c) D/C 1:5.

solution were characterized by partially fused and interconnected fibers. Furthermore, a preliminary investigation about the effect of the increasing amount of DMF (PPeF D/C (1/5) sample) for electrospinning of the PPeF solution can be appreciated by the FESEM images acquired that highlight the importance of the working temperature but also the solvents used. On the other hand, the PBF mats showed smooth and homogeneous fibers, which might be due to the semicrystalline nature of PBF in contrast with the fully amorphous nature of PPeF. The best results obtained under controlled temperature and humidity, in terms of homogeneity and the submicrometric dimension of the PBF fibers, were

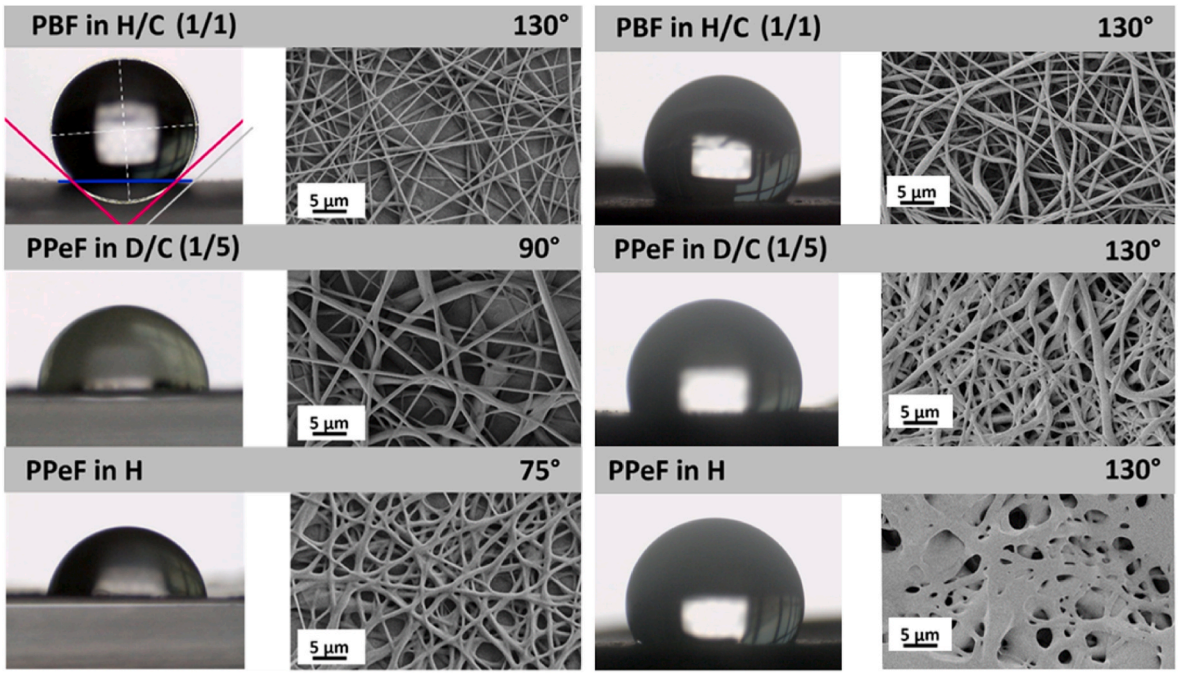

Fig. 7. Representative image of the contact angle analysis of a water drop on optimized PBF and PPeF electrospun mats. Left column: as-prepared mats; right column: mats dried under vacuum overnight.

obtained at 0.11 g/mL, 24 kV, and 0.01 mL/min in a solvent mixture of H/C (1/1). Whereas, PPeF mats with good microstructural quality were obtained under the following conditions: PPeF 0.2 g/mL, 24 kV, 0.1 mL/min in a solvent mixture of D/C (1/5) or 0.05 mL/min in HFIP at 0.1 g/mL. Furthermore, the WCA analysis highlighted the hydrophobicity of PPeF and PBF mats after the complete removal of the solvent.

These results are very promising for the application of these PBF and PBF electrospun nanofibrous mats in the biomedical field. However, their suitability as biomedical devices cannot be ensured without cytotoxicity tests and the evaluation of their mechanical performance; these two tests are the object of upcoming work.

CRediT authorship contribution statement

Sofia Santi: Conceptualization, Data curation, Formal analysis, Investigation, Methodology, Validation, Visualization, Writing – original draft, Writing – review & editing. **Michelina Soccio:** Conceptualization, Data curation, Funding acquisition, Investigation, Methodology, Validation, Writing – review & editing. **Giulia Fredi:** Conceptualization, Data curation, Funding acquisition, Methodology, Validation, Writing – review & editing. **Nadia Lotti:** Conceptualization, Funding acquisition, Methodology, Project administration, Resources, Supervision, Writing – review & editing. **Andrea Dorigato:** Conceptualization, Funding acquisition, Project administration, Resources, Supervision, Writing – review & editing.

Declaration of competing interest

The authors declare the following financial interests/personal relationships which may be considered as potential competing interests: Sofia Santi, Giulia Fredi, and Andrea Dorigato report financial support was provided by Trento and Rovereto Bank Foundation. Nadia Lotti and Michelina Soccio report financial support was provided by European Cooperation in Science and Technology.

Data availability

Data will be made available on request.

Acknowledgements

This research activity has been funded by Cassa di Risparmio di Trento and Rovereto (CARITRO) within the project “studio di una nuova generazione di bioplastiche a base di poliesteri furanoati per packaging e fibre tessili sostenibili (BioPackTex)”, grant number 2020.0265. M.S. and N.L. also acknowledge the Italian Ministry of University and Research. This publication is based upon work from COST Action FUR4Sustain, CA18220, supported by COST (European Cooperation in Science and Technology).

References

[1] C. Fosse, A. Bourdet, E. Ernault, A. Esposito, N. Delpouve, L. Delbreilh, S. Thiyagarajan, R.J.I. Knoop, E. Dargent, Thermochim. Acta 677 (2019) 67.
[2] M. Shen, B. Song, G. Zeng, Y. Zhang, W. Huang, X. Wen, W. Tang, Environ. Pollut. (2020) 263.
[3] S. Nanda, B.R. Patra, R. Patel, J. Bakos, A.K. Dalai, Environ. Chem. Lett. 20 (2022) 379–395.
[4] F. Anna, Plastic Waste: Here’s what it Could Look like by 2060, 2022. https://www.weforum.org/agenda/2022/07/recycling-efforts-not-enough-to-solve-plastic-waste-problem/.
[5] A. Dorigato, D. Perin, A. Pegoretti, J. Polym. Environ. 28 (2020) 3244.
[6] F. Valentini, A. Dorigato, D. Rigotti, A. Pegoretti, J. Polym. Environ. 27 (2019) 1333–1341.
[7] A. Dorigato, M. Negri, A. Pegoretti, J Renew Mater 6 (2018) 493–503.
[8] A. Dorigato, M. Negri, A. Pegoretti, Polym. Compos. 39 (2018) 1116.
[9] Bioplastics Market Data, 2022. https://www.european-bioplastics.org/market/.
[10] M. Soccio, D.E. Martínez-Tong, G. Guidotti, B. Robles-Hernández, A. Munari, N. Lotti, A. Alegria, Polymers 12 (2020).
[11] G. Guidotti, M. Soccio, N. Lotti, V. Siracusa, M. Gazzano, A. Munari, Polym. Degrad. Stabil. 169 (2019).
[12] M. Soccio, N. Lotti, A. Munari, E. Rebollar, D.E. Martínez-Tong, Polymer (2020) 202.
[13] G. Guidotti, M. Soccio, N. Lotti, M. Gazzano, V. Siracusa, A. Munari, Polymers 10 (2018).
[14] J. Ma, X. Yu, J. Xu, Y. Pang, Polymer 53 (2012) 4145.
[15] M. Soccio, M. Costa, N. Lotti, M. Gazzano, V. Siracusa, E. Salatelli, P. Manaresi, A. Munari, Eur. Polym. J. 81 (2016) 397.
[16] F.A. Kucherov, E.G. Gordeev, A.S. Kashin, V.P. Ananikov, Angew. Chem. 129 (2017), 16147.
[17] G.Z. Papageorgiou, D.G. Papageorgiou, Z. Terzopoulou, D.N. Bikiaris, Eur. Polym. J. 83 (2016) 202–229.
[18] V. Tsanaktsis, D.G. Papageorgiou, S. Exarhopoulos, D.N. Bikiaris, G. Z. Papageorgiou, Cryst. Growth Des. 15 (2015) 5505.

[19] J.G. Rosenboom, D.K. Hohl, P. Fleckenstein, G. Storti, M. Morbidelli, Nat. Commun. 9 (2018).
[20] A. Gandini, A.J.D. Silvestre, C.P. Neto, A.F. Sousa, M. Gomes, J. Polym. Sci. Polym. Chem. 47 (2009) 295.
[21] M. Soccio, D.E. Martínez-Tong, A. Alegría, A. Munari, N. Lotti, Polymer 128 (2017) 24.
[22] E. Bianchi, M. Soccio, V. Siracusa, M. Gazzano, S. Thiyagarajan, N. Lotti, ACS Sustain. Chem. Eng. 9 (2021), 11937.
[23] S. Quattrosoldi, G. Guidotti, M. Soccio, V. Siracusa, N. Lotti, Chemosphere 291 (2022), 132996.
[24] D.E. Martínez-Tong, M. Soccio, B. Robles-Hernández, G. Guidotti, M. Gazzano, N. Lotti, A. Alegria, Macromolecules 53 (2020), 10526.
[25] G. Guidotti, M. Soccio, M.C. García-Gutiérrez, E. Gutiérrez-Fernández, T. A. Ezquerra, V. Siracusa, A. Munari, N. Lotti, ACS Sustain. Chem. Eng. 7 (2019), 17863.
[26] J. Zhu, J. Cai, W. Xie, P.H. Chen, M. Gazzano, M. Scandola, R.A. Gross, Macromolecules 46 (2013) 796.
[27] D. Perin, G. Fredi, D. Rigotti, M. Soccio, N. Lotti, A. Dorigato, J. Appl. Polym. Sci. (2022) 139.
[28] G. Guidotti, M. Soccio, M.C. García-Gutiérrez, T. Ezquerra, V. Siracusa, E. Gutiérrez-Fernández, A. Munari, N. Lotti, ACS Sustain. Chem. Eng. 8 (2020) 9558.
[29] D. Perin, D. Rigotti, G. Fredi, G.Z. Papageorgiou, D.N. Bikiaris, A. Dorigato, J. Polym. Environ. 29 (2021) 3948.
[30] D. Rigotti, M. Soccio, A. Dorigato, M. Gazzano, V. Siracusa, G. Fredi, N. Lotti, ACS Sustain. Chem. Eng. 9 (2021), 13742.
[31] S. Guo, Q. Ke, H. Wang, X. Jin, Y. Li, J. Appl. Polym. Sci. 128 (2013) 3652.
[32] D.L. Puhl, J.L. Funnell, D.W. Nelson, M.K. Gottipati, R.J. Gilbert, Bioengineering 8 (2021) 1–34.
[33] B. Robb, B. Lennox, in: Electrospinning for Tissue Regeneration, Elsevier, 2011, p. 51.
[34] T. Uyar, F. Besenbacher, Polymer 49 (2008) 5336.
[35] P. Stagnaro, G. Luciano, R. Utzeri. https://moodle2.units.it/pluginfile.php/283832/mod_resource/content/1/Appunti-%20DSC-TGA.pdf.
[36] A.C. Drake, Y. Lee, E.M. Burgess, J.O.M. Karlsson, A. Eroglu, A.Z. Higgins, PLoS One 13 (2018).
[37] B.K. Raghavan, D.W. Coffin, J. Eng. Fibers. Fabr. 6 (4) (2011).
[38] John Burke, The Book and Paper Group, Volume 3. https://cool.cultural heritage.org/byauth/burke/solpar/.
[39] M.L. Cheng, C.C. Lin, H.L. Su, P.Y. Chen, Y.M. Sun, Polymer 49 (2008) 546.
[40] R.M. Nezarati, M.B. Eifert, E. Cosgriff-Hernandez, Tissue Eng. C Methods 19 (2013) 810.
[41] A. Pegoretti, A. Dorigato, M. Brugnara, A. Penati, Eur. Polym. J. 44 (2008) 1662–1672.